

Dear Editor and Reviewers,

We would like to express our sincere appreciation for your handling of our manuscript and for the valuable comments and suggestions offered. We have carefully considered the comments and have revised the manuscript accordingly. The comments are laid out below in italicized font. Our response is given in normal font and changes/additions to the manuscript are given in the blue text.

Responses to reviewer one's comments

1. *#I greatly appreciate the authors' responses and the substantial revisions made to the manuscript. The authors have addressed most of my questions; however, the Discussion section still requires improvement, as it remains insufficiently in-depth. Although an additional section has been added, it consists almost entirely of limitations and does not place the results in the context of other relevant studies. This considerably diminishes the perceived novelty or significance of the paper. In a word, the authors need to provide more detailed discussion (at least one aspect) rather than relying on a general statement such as: "Crucially, this methodological framework is transferable. For application in other tectonic regions, the model can be adapted by similarly optimizing the parameter combinations for the target hot springs based on their specific hydrochemical components." In this case, the methods and data in this paper are too local, and explaining how they can be applied to other studies or regions, with a more specific discussion on at least one aspect, even if only one additional sentence is added, would greatly improve the paper.*

Response: We sincerely thank the reviewer for the constructive feedback. We recognize that the previous version lacked a comprehensive context and tangible guidance for transferability. To address your concern, we have substantially revised the Discussion section to place our findings in the context of other relevant global studies.

We have completely overhauled this part on lines 553-571 as follows:

Although the specific parameters in this study are local, the underlying method framework could be transferable when specific selection criteria for monitoring sites are met. Monitoring stations should be situated in active tectonic regions, such as western Türkiye (Yakupoglu et al., 2025), or even at major fault intersections, such as XJF and RRF intersection zone (Shao et al., 2024). Priority should be given to high-temperature, deep-circulated thermal springs, as their hydrochemical components carry deep-seated information while minimizing interference from meteoric water. Furthermore, the hydrogeochemical background of the spring must be clearly defined to distinguish its hydrogeochemical characteristics from shallow water bodies and to monitor mixing processes. Springs with a long observation duration, where historical earthquakes have induced data oscillations, should be prioritized. According to findings in Iceland (Skelton et al., 2024), these oscillatory signals originate from the physical coupling of crustal dilation and fracture mineralization, representing a reliable geochemical signature during the stress build-up phase. Preference is also given to springs with bubbling gases to expand gas-chemical observations. Additionally, sites that could incorporate specific crustal deformation-sensitive isotopic monitoring indicators are ideal, such as He isotopes in the Noto Peninsula (Kagoshima et al., 2025) or H-O-C isotopes in the Xianshuihe fault (Yu et al., 2026). Our model can be practically applied to platforms such as the China Seismic Experimental Site (CSES) and the European Plate Observing System (EPOS), where the future of earthquake forecasting depends on multiple-method synergy. For instance, cross-validating hydrochemical anomalies with b-value evaluation (Chang et al., 2025), ionospheric TEC (Baselga, 2024), or load/unload response ratio and outgoing longwave radiation coupling (Lei et al., 2024) establishes a robust, multi-layered verification process. Within this hierarchical system, broad-scale geophysical tools effectively flag regional risks. Conversely, our site-specific, multi-component hydrochemical model provides the confirmation necessary for small-scale, short-term forecasting.

References:

Baselga, S.: Artificial Intelligence for Earthquake Prediction: A Preliminary System Based on Periodically Trained Neural Networks Using Ionospheric Anomalies, *Applied Sciences*, 14, 10895, <https://doi.org/10.3390/app142310859>, 2024.

Chang, Y., Wang, R., Han, P., Wang, J., Miao, M., Zeng, Z., Wu, W., Jiang, C., Meng, L., Shi, H., and Hattori, K.: b-Value Evaluation and Applications to Seismic Hazard Assessment, *Entropy*, 27, 958. <https://doi.org/10.3390/e27090958>, 2025.

Kagoshima, T., Sano, Y., Takahata, N., Kawamoto, Y., Shibata, T., Li, Y., Morishita, T., Hiramatsu, Y., and Nakajima, J.: Helium isotope anomaly in groundwater prior to the 2024 Noto Peninsula earthquake, *Nature Communications*, 16(1), 10414. <https://doi.org/10.1038/s41467-025-65717-9>, 2025.

Lei, Y., Jianyong, L., Chen, Y., Haizhen, Z., Dequan, H., and Weiyu, M.: Determination of stress state based on coupling characteristics of load/unload response ratio and outgoing longwave radiation before large earthquakes, *Frontiers in Earth Science*, 12: 1433395, <https://doi.org/10.3389/feart.2024.1433395>, 2024.

Shao, W., Liu, Z., Li, Y., Chen, Z., Lu, C., Zhao, C., Wang, Y., Li, Q., Gao, Z., Luo, Y., Ran, H., and Fan, S.: Geochemical Characteristics of Thermal Springs and Insights Into the Intersection Between the Xiaojiang Fault and the Red River Fault, Southeastern Tibet Plateau, *Geochemistry, Geophysics, Geosystems*, 25(3), <https://doi.org/10.1029/2023gc011431>, 2024.

Skelton, A., Sturkell, E., Mörth, C.-M., Stockmann, G., Jónsson, S., Stefansson, A., Liljedahl-Claesson, L., Wästeby, N., Andrén, M., Tollefsen, E., Gunnarsson Robin, J., Keller, N., Geirsson, H., Hjartarson, H., and Kockum, I.: Towards a method for forecasting earthquakes in Iceland using changes in groundwater chemistry, *Communications Earth & Environment*, 5(1), <https://doi.org/10.1038/s43247-024-01852-3>, 2024.

Yakupoğlu, N., Sabuncu, A., Erbil, C., Kirkan E., Çetin H., and İnan S.: Pre-earthquake hydrogeochemical anomalies in spring waters: two distinctive cases from

western Türkiye, Journal of Hydrology, 662,
<https://doi.org/10.1016/j.jhydrol.2025.133920>, 2025.

Yu, Y., Song, H., Liang, J., Liu, X., Luo, Z., Zhao, J., Li, Z., and Xu, J.: The evidence of H-O-C isotopes in response to earthquake and the precursor anomaly index: A case study of geothermal fluids in the Xianshuihe fault, Geothermics, 134, <https://doi.org/10.1016/j.geothermics.2025.103491>, 2026.

Responses to reviewer three's comments

1. *#The study would be strengthened with an analysis and discussion of whether considering the directions (increase or decrease) of the identified multicomponent change points helps with the event identification. Considering abnormal increases and decreases as equivalent in event detection is a simple but not well justified choice. The discussion in lines 346 to 360 implies that the direction of the change point is related to the mechanisms of the ion concentration responses, and can contribute to event prediction. For instance, it suggests that an anomalous increase in ^{18}O might be more related to an upcoming earthquake compared to a decrease in ^{18}O . This additional analysis will set this paper part from existing literature on change point analysis of time series anomalies.*

Response: We thank the reviewer for this insightful comment. We completely agree that the direction of anomalous variations (increase vs. decrease) is crucial for understanding the response mechanisms and enhancing event identification. In response to your suggestion, we performed a detailed statistical analysis of the anomaly directions for 9 components across the two hot springs (Table 1). During our analysis, we observed that certain pre-seismic anomalies manifest as intense bidirectional fluctuations. Currently, there is a lack of a criterion to define a “dominant direction” for such oscillatory signals. Our initial statistics indicate that anomalous increases (57%~77%) are more frequent than decreases for most ions (e.g., Na^+ , Cl^- , SO_4^{2-}). While these findings provide tentative support for the assume that “increases” possess a stronger correlation with seismic events, the current sample size and statistical depth remain exploratory. Additionally, as the reviewer noted regarding δD and $\delta^{18}\text{O}$, our statistics show that these components exhibit a higher frequency of decreases (60%~75%), and change directions can vary across different components for the same earthquake event. Such divergence between different components suggests that a simplistic, unidirectional criterion might overlook vital precursor information. Based on these findings, our existing detection model is primarily oriented toward identifying

sustained positive anomalies (i.e., anomalous increases), while also accounting for recovery phases following a decline (i.e., the increase following an anomalous decrease). Nevertheless, despite our best efforts, directly incorporating these specific directional variations into earthquake forecasting remains a challenge at this stage.

Table 1. Statistical analysis of anomalous variations in hydrochemical components.

Ion	Qujiang spring				Wana spring			
	Increase (<i>n</i>)	Decrease (<i>n</i>)	Increase Ratio	Decrease Ratio	Increase (<i>n</i>)	Decrease (<i>n</i>)	Increase Ratio	Decrease Ratio
Na ⁺	10	4	0.71	0.29	3	1	0.75	0.25
K ⁺	8	4	0.67	0.33	3	2	0.60	0.40
Ca ²⁺	10	6	0.63	0.38	4	5	0.44	0.56
Cl ⁻	11	7	0.61	0.39	6	3	0.67	0.33
SO ₄ ²⁻	10	3	0.77	0.23	5	5	0.50	0.50
HCO ₃ ⁻	6	4	0.60	0.40	5	2	0.71	0.29
F ⁻	11	4	0.73	0.27	4	3	0.57	0.43
δD	1	3	0.25	0.75	2	3	0.40	0.60
δ ¹⁸ O	1	2	0.33	0.67	2	3	0.40	0.60

2. *#What is the justification for using the functional form $p5^M$ for the alert period? Please support it with literature.*

Response: We sincerely thank the reviewer for pointing this out. First, we would like to clarify a slight misunderstanding regarding the definition of this period in our algorithm. The term $p5^M$ represents the post-alert threshold adjustment period (the duration of the anomaly following a successful alert and subsequent earthquake). During this specific period, the algorithm temporarily raises the warning thresholds to suppress redundant false alarms caused by post-earthquake disturbances and ongoing continuous anomalies.

Numerous studies have demonstrated that the duration of earthquake-related anomalies (T) exhibits an exponential relationship with the earthquake magnitude (M). This is commonly expressed in a logarithmic form, such as $\log T = aM + b$, which mathematically translates to $T = 10^b \times (10^a)^M$. Rikitake (1988) established the

relationship $\log T = 0.76M - 1.83$ for precursor anomaly durations. Fleischer et al. (1985) utilized the relation $M = 2\log T - 0.07$ for Rn anomaly durations. Ilić et al. (2005) and Elmaghraby et al. (2009) similarly demonstrated logarithmic relationships between magnitude and anomaly duration across various detection methods and regions. Therefore, we adopted the generalized exponential form $p5^M$. By leaving the base as an optimized parameter ($p5$), the algorithm is able to dynamically identify the best-fitting exponential base for the specific regional data being analyzed, ensuring maximum algorithmic adaptability.

We have revised the manuscript on line 276 to clarify the purpose of this period and to include the relevant literature justifying the mathematical form:

Following an earthquake, the algorithm enters a post-earthquake threshold adjustment period to suppress redundant false alarms caused by ongoing post-earthquake anomalies, new parameters $p1' = p4 \times p1$ and $p3' = p4 \times p3$ are used for a period of $p5^M$ (where M is the magnitude). The functional form $p5^M$ is adopted based on an exponential relationship between earthquake magnitude and geochemistry anomaly duration (Fleischer et al., 1985; Rikitake, 1988; Elmaghraby et al., 2009). Treating the base $p5$ as a tunable parameter allows the algorithm to dynamically optimize this duration for specific regional data. If subsequent earthquakes occur within this period, the post-earthquake time is calculated based on the maximum magnitude of the subsequent earthquakes.

References:

Elmaghraby E. K., Lotfy Y. A.: Differentiation between earthquake radon anomalies and those arising from nuclear activities, *Applied Radiation and Isotopes*, 67(1): 208-211, <https://doi.org/10.1016/j.apradiso.2008.07.003>, 2009.

Fleischer L. F., Mogro-Campero A.: Association of subsurface radon changes in Alaska and the northeastern United States with earthquakes, *Geochimica et Cosmochimica Acta*, 49(4): 1061-1071, [https://doi.org/10.1016/0016-7037\(85\)90319-9](https://doi.org/10.1016/0016-7037(85)90319-9), 1985.

Ilić R., Rusov V. D., Pavlovych V. N., Vaschenko V. M., Hanžič L., Bondarchuk

Y.A.: Radon in Antarctica, Radiation Measurements, 40(2-6): 415-422, <https://doi.org/10.1016/j.radmeas.2005.03.022>, 2005.

Rikitaket: Earthquake prediction: an empirical approach, tectonophysics, 148(3-4): 19-210, [https://doi.org/10.1016/0040-1951\(88\)90128-x](https://doi.org/10.1016/0040-1951(88)90128-x), 1988.

3. *#Line 544: To improve conclusion 1, analyze the data to check whether it is possible to identify a response time that is dependent on earthquake size, instead of a uniform 45 day period for all earthquake events.*

Response: Thank you for this insightful suggestion. We agree that, theoretically, the physical preparation process and seismic response time threshold may vary depending on the magnitude. However, our correlation analysis confirms that a uniform threshold is both statistically supported and operationally necessary for the anomaly detection model. As illustrated in the scatter plot of magnitude (M) versus response time (T_{th}), there is no discernible linear or monotonic relationship between these variables, with T_{th} remaining highly dispersed (ranging from 0 to 60 days) regardless of magnitude for all events where $M \geq 4.0$. Even for multiple seismic events of the identical magnitude, the observed T_{th} remain inconsistent. These suggest that the T_{th} is likely governed by complex local tectonic settings and stress accumulation states rather than earthquake magnitude alone.

Notably, from a practical forecasting perspective, the magnitude of a pending earthquake is an unknown variable, meaning a magnitude-dependent threshold could only be applied after the event has occurred, which would render the model unusable for real-time applications. Furthermore, cross-correlation, BCP analysis, and parameter

optimization consistently identify 45 days pre-earthquake as the T_{th} . Therefore, we have maintained the uniform 45-day window as a statistically optimized best-fit threshold that captures the maximum number of true positive correlations for all $M \geq 4.0$ events while ensuring the model's practical utility in actual forecasting scenarios.

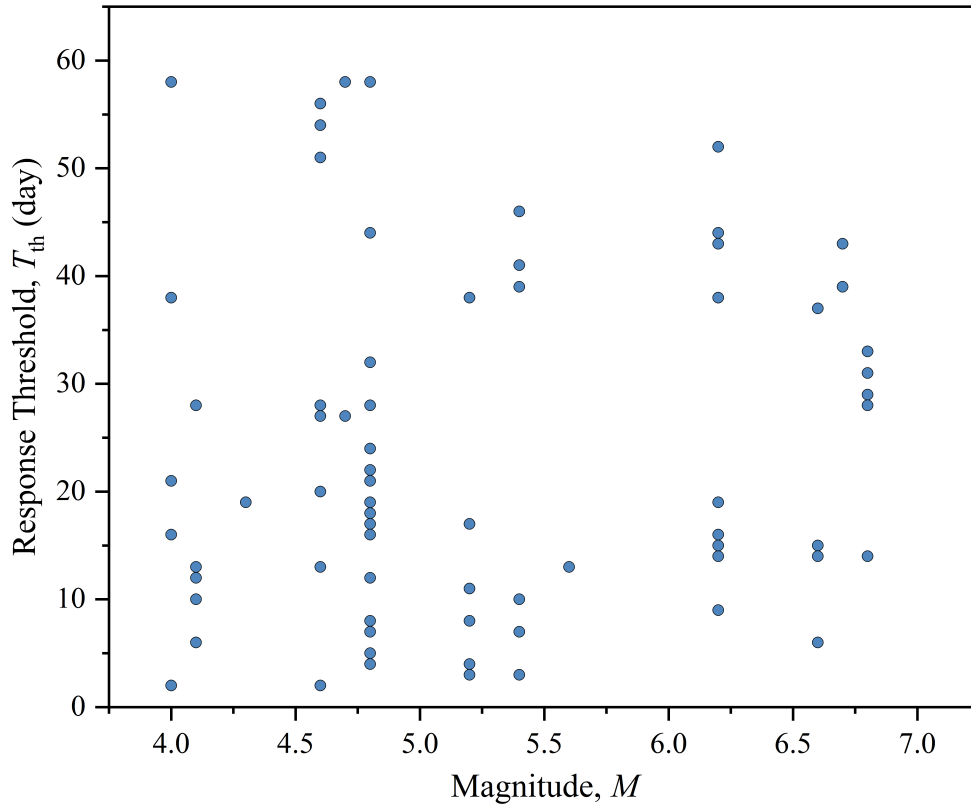


Figure 1. Scatter plot of earthquake magnitude (M) versus seismic response time threshold (T_{th}).

4. *#The limitations section does not provide depth in discussion. The parts between lines 518 to 536 are too generic and should be shortened. Additional discussion on the limitations of this study, with detailed comparisons with other alternative earthquake forecasting methods, including other multiparameter/multicomponent methods, is necessary. Additional discussion of how the current method can be complementarily used with other forecasting methods is also useful.*

Response: We sincerely thank the reviewer for the constructive critique. We agree that the previous discussion on limitations was somewhat generic. In the revised manuscript, we have significantly condensed the original general statements and replaced them with a case-driven analysis of limitations and prospects, coupled with a comparison with alternative forecasting methods. We have completely overhauled this part on lines 537-571 as follows:

Approximately 30 days after the last synchronized false alarms at the two thermal springs (Figures 7 and 8), an $M4.1$ earthquake occurred outside the expected preparation zone. This highlights another key limitation: the current algorithm relies on an effective and widely used isotropic underground structure assumption, and exhibits limited adaptability to long-term data trends, dictating the need for periodic parameter re-optimization.

Despite these constraints, the multi-component anomaly detection model developed here demonstrates robust performance, achieving an accuracy exceeding 83% and a TS ranging from 59% to 70%. These metrics are highly consistent with the positive predictive values of 62% to 85% reported by Skelton et al. (2024) using δD and $\delta^{18}O$ sequences in Iceland. In the context of cross-disciplinary forecasting, the efficacy of our approach remains competitive compared to the 73.82% accuracy achieved by Mukherjee et al. (2025) through machine learning with multiple seismological features, and the approximately 60% accuracy reported by Baselga (2024) for ionospheric anomaly forecasting. Within the field of geochemical forecasting, our results compare favorably with the 71% accuracy for radon anomalies obtained by Feng et al. (2022) and the 70% accuracy for multi-parameter hydrochemical detection described by Zhu et al. (2024) using the LOF algorithm. By leveraging the differentiated responses of various components to crustal stress, our synergistic analysis significantly enhances the identification of subtle pre-earthquake signals. Mechanistically, this multi-indicator integration provides a more objective reflection of pre-earthquake stress changes and fluid mixing processes and higher advantages in filtering environmental interference, consistent with the tectonic stress drivers

discussed by Yakupoğlu et al. (2025).

Although the specific parameters in this study are local, the underlying method framework could be transferable when specific selection criteria for monitoring sites are met. Monitoring stations should be situated in active tectonic regions, such as western Türkiye (Yakupoğlu et al., 2025), or even at major fault intersections, such as XJF and RRF intersection zone (Shao et al., 2024). Priority should be given to high-temperature, deep-circulated thermal springs, as their hydrochemical components carry deep-seated information while minimizing interference from meteoric water. Furthermore, the hydrogeochemical background of the spring must be clearly defined to distinguish its hydrogeochemical characteristics from shallow water bodies and to monitor mixing processes. Springs with a long observation duration, where historical earthquakes have induced data oscillations, should be prioritized. According to findings in Iceland (Skelton et al., 2024), these oscillatory signals originate from the physical coupling of crustal dilation and fracture mineralization, representing a reliable geochemical signature during the stress build-up phase. Preference is also given to springs with bubbling gases to expand gas-chemical observations. Additionally, sites that could incorporate specific crustal deformation-sensitive isotopic monitoring indicators are ideal, such as He isotopes in the Noto Peninsula (Kagoshima et al., 2025) or H-O-C isotopes in the Xianshuihe fault (Yu et al., 2026). Our model can be practically applied to platforms such as the China Seismic Experimental Site (CSES) and the European Plate Observing System (EPOS), where the future of earthquake forecasting depends on multiple-method synergy. For instance, cross-validating hydrochemical anomalies with b-value evaluation (Chang et al., 2025), ionospheric TEC (Baselga, 2024), or load/unload response ratio and outgoing longwave radiation coupling (Lei et al., 2024) establishes a robust, multi-layered verification process. Within this hierarchical system, broad-scale geophysical tools effectively flag regional risks. Conversely, our site-specific, multi-component hydrochemical model provides the confirmation necessary for small-scale, short-term forecasting.

References:

Baselga, S.: Artificial Intelligence for Earthquake Prediction: A Preliminary System Based on Periodically Trained Neural Networks Using Ionospheric Anomalies, *Applied Sciences*, 14, 10895, <https://doi.org/10.3390/app142310859>, 2024.

Chang, Y., Wang, R., Han, P., Wang, J., Miao, M., Zeng, Z., Wu, W., Jiang, C., Meng, L., Shi, H., and Hattori, K.: b-Value Evaluation and Applications to Seismic Hazard Assessment, *Entropy*, 27, 958. <https://doi.org/10.3390/e27090958>, 2025.

Feng, X., Zhong, J., Yan, R., Zhou, Z., Tian, L., Zhao, J., and Yuan, Z.: Groundwater Radon Precursor Anomalies Identification by EMD-LSTM Model, *water*, 14(1), <https://doi.org/10.3390/w14010069>, 2022.

Kagoshima, T., Sano, Y., Takahata, N., Kawamoto, Y., Shibata, T., Li, Y., Morishita, T., Hiramatsu, Y., and Nakajima, J.: Helium isotope anomaly in groundwater prior to the 2024 Noto Peninsula earthquake, *Nature Communications*, 16(1), 10414. <https://doi.org/10.1038/s41467-025-65717-9>, 2025.

Lei, Y., Jianyong, L., Chen, Y., Haizhen, Z., Dequan, H., and Weiyu, M.: Determination of stress state based on coupling characteristics of load/unload response ratio and outgoing longwave radiation before large earthquakes, *Frontiers in Earth Science*, 12: 1433395, <https://doi.org/10.3389/feart.2024.1433395>, 2024.

Mukherjee, B., Shaw, R. L., Sharma, M. L., and Sain, K.: Earthquake prediction using machine learning perspectives in Himalayan seismic belt and its surroundings, *Journal of Asian Earth Sciences*, 293, <https://doi.org/10.1016/j.jseaes.2025.106764>, 2025.

Shao, W., Liu, Z., Li, Y., Chen, Z., Lu, C., Zhao, C., Wang, Y., Li, Q., Gao, Z., Luo, Y., Ran, H., and Fan, S.: Geochemical Characteristics of Thermal Springs and Insights Into the Intersection Between the Xiaojiang Fault and the Red River Fault, Southeastern Tibet Plateau, *Geochemistry, Geophysics, Geosystems*, 25(3), <https://doi.org/10.1029/2023gc011431>, 2024.

Skelton, A., Sturkell, E., Mörth, C.-M., Stockmann, G., Jónsson, S., Stefansson, A., Liljedahl-Claesson, L., Wästeby, N., Andrén, M., Tollefsen, E., Gunnarsson Robin,

J., Keller, N., Geirsson, H., Hjartarson, H., and Kockum, I.: Towards a method for forecasting earthquakes in Iceland using changes in groundwater chemistry, *Communications Earth & Environment*, 5(1), <https://doi.org/10.1038/s43247-024-01852-3>, 2024.

Yakupoglu, N., Sabuncu, A., Erbil, C., Kirkan E., Çetin H., and İnan S.: Pre-earthquake hydrogeochemical anomalies in spring waters: two distinctive cases from western Türkiye, *Journal of Hydrology*, 662, <https://doi.org/10.1016/j.jhydrol.2025.133920>, 2025.

Yu, Y., Song, H., Liang, J., Liu, X., Luo, Z., Zhao, J., Li, Z., and Xu, J.: The evidence of H-O-C isotopes in response to earthquake and the precursor anomaly index: A case study of geothermal fluids in the Xianshuihe fault, *Geothermics*, 134, <https://doi.org/10.1016/j.geothermics.2025.103491>, 2026.

Zhu, R., Yang, F., Zhou, X., Tian, J., Zhang, Y., He, M., Li, J., Dong, J., and Li, Y.: Anomaly Detection Using Machine Learning in Hydrochemical Data From Hot Springs: Implications for Earthquake Prediction, *Water Resources Research*, 60(6), <https://doi.org/10.1029/2023wr034748>, 2024.

5. *#The figure for the anomaly detection algorithm (figure S4) would be better placed in the manuscript instead of the supplementary material.*

Response: Thank! We agree that the anomaly detection algorithm is central to the methodology described in this study. Accordingly, we have moved Figure S4 (now Figure 4) from the Supplementary Material to the manuscript to provide better clarity and immediate access for the reader

6. *#The meaning of “This study modifies the algorithmic workflow to a backward processing mode, enabling real-time forward forecasting” in line 257 is not clear. What does backward processing mean, and what does it contrast with? Surely the opposite “forward processing” is not possible because future data has not been*

observed yet at the point of forecast.

Response: Thank you for this insightful comment. We understand that the term ‘backward processing’ may cause ambiguity. To clarify, ‘backward processing’ in this study refers to a look-back mechanism where the algorithm analyzes a window of historical data in reverse-chronological order (from t back to $t-n$) to establish a dynamic threshold. To ensure clarity, we have revised this sentence in the updated manuscript on line 257:

This study optimizes the algorithmic workflow by retrospectively analyzing data in reverse-chronological order to establish dynamic thresholds, enabling real-time forecasting

7. *#Line 496-503: Can these trends be quantified with some kind of regression and visualized with a figure?*

Response: Thank you for your valuable suggestion. We have quantified and visualized the relationship between the number of synchronous anomalous components (Y), earthquake magnitude (M), and epicentral distance (Δ). A critical finding is the robust linear scaling relationship between magnitude and distance for significant events ($Y \geq 6$), which can be expressed as $M = 0.007\Delta + 4.03$ ($R = 0.85$, $P = 0.004$). To comprehensively quantify and visualize all the events, we have categorized the earthquake events based on a magnitude threshold of $M = 6.0$, this analysis allows for a deeper understanding of the distinct "Distance-dominant" and "Magnitude-dominant" trends observed in our data. We have created a new figure (Figure 11) to illustrate these findings. Correspondingly, we have made the following revisions on line 500 in the revised manuscript:

Spatially, the number of hydrochemical components (Y) exhibiting synchronous anomalies correlates with earthquake magnitude and epicentral distance (Figure 11). Earthquakes that induce synchronous anomalies in six or more hydrochemical components have epicentral distances of less than 150 km for earthquakes with

magnitudes less than 6.0 ($M < 6.0$), while this distance extends to approximately 400 km for earthquakes with magnitudes greater than or equal to 6.0 ($M \geq 6.0$). Among these significant events ($Y \geq 6$), a robust linear correlation exists between magnitude and distance ($R = 0.85$, $P = 0.004$). This correlation provides a quantitative basis for seismic risk assessment, allowing for the estimation of a potential earthquake's minimum magnitude or its maximum likely distance based on observed hydrochemical precursors.

Although it is difficult to quantify the exact impact of magnitude and distance on the number of components exhibiting synchronous anomalies, as magnitude increases or distance decreases, the number of components with synchronous anomalies detected by the model tends to increase. Especially, the result reveals a distinct delineation in trend at the $M = 6.0$ threshold. For earthquakes where $M < 6.0$, the number of anomalous components is primarily sensitive to epicentral distance; shorter distances yield a higher count of synchronous anomalous components due to proximity to the stress-release center. For earthquakes where $M \geq 6.0$, the influence of distance diminishes significantly. In this regime, magnitude becomes the primary driver, as high-energy release can trigger regional-scale crustal stress perturbations that induce hydrochemical anomalies even at remote distances. This trend aligns with the positive correlation between the scale of earthquake energy release and the number of anomalies, as confirmed by the hydrochemical monitoring results (Li et al., 2022). Therefore, a significant relationship is present between the temporal variation of hydrochemical components and earthquakes in the study region. The number of components exhibiting synchronous anomalies can be used as an effective criterion for determining alarm intensity, with higher intensity generally corresponding to larger earthquake magnitudes or shorter epicentral distances.

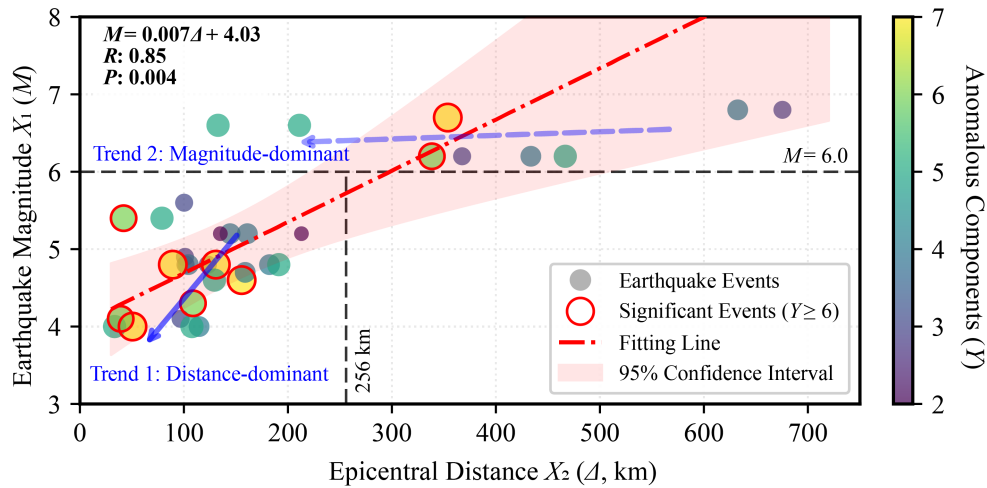


Figure 11: Relationship between the number of synchronous anomalous hydrochemical components, earthquake magnitude, and epicentral distance.

8. #Abstract: One of the sites has only 3 years of data, not 5. The abstract should specify the number of total, predicted, missed, and false alarms within the monitoring period, separately for each of the two sites. The abstract should also state that the alarm criteria is adaptive because changes for a short time after an earthquake is observed. Clarify what is meant by alarm intensity in the abstract.

Response: Thank! We have revised the abstract and conclusions as follows:

Abstract. The intersection of the Xiaojiang Fault and the Red River Fault at the southeastern margin of the Tibetan Plateau encounters intense tectonic activity, where repeated earthquakes cause variations in thermal spring hydrochemistry. This study applies Bayesian change point analysis and develops a multi-component synergetic anomaly detection model, using monitoring data from the Qujiang (5 years, 2019–2024) and Wana (2.5 years, 2021–2024) springs in this region to facilitate the real-time forecasting of the occurrence timing for $M \geq 4$ earthquakes. A 45-day response time threshold is established as the optimal period for capturing critical hydrochemical precursors associated with $M \geq 4$ earthquakes. With parameters optimized for individual components based on their distinct geochemical responses to seismic stress, the model features adaptive alarm criteria that ensure reliable real-time detection and enhanced

adaptability. At the Qujiang site, the model achieved 21 effective alarms for 22 earthquake events with 1 miss and 8 false alarms, yielding a probability of detection (POD) of 0.95 and a threat score (TS) of 0.70. At the Wana site, the model generated 10 accurate alarms for 12 events with 2 misses and 5 false alarms, resulting in a POD of 0.83 and a TS of 0.59. It identified pre-earthquake anomalies in Na^+ , Ca^{2+} , Cl^- , SO_4^{2-} , δD , and $\delta^{18}\text{O}$, with $\text{TS} \geq 0.50$, which can serve as sensitive indicators for strong earthquake forecasting. The multicomponent *synergetic* alarm mechanism for hydrochemistry overcomes the limitations of single-parameter methods, using the number of hydrochemical components with synchronous anomalies serves as a reliable criterion for forecasting, a higher count of anomalous components typically correlating with larger earthquake magnitudes or shorter epicentral distances. This model can be universally applied to thermal spring monitoring across diverse tectonic regions through targeted parameter optimisation, offering a valuable reference for earthquake forecasting.

Conclusion on line 583:

The anomaly detection model features adaptive alarm criteria and demonstrates reliable real-time anomaly detection capabilities, yielding a POD of 0.95 and a TS of 0.70 at the QJ site, whereas the WN site maintains a POD of 0.83 and a TS of 0.59.

Conclusion on line 591:

The number of hydrochemical components with synchronous anomalies provides a reliable criterion for forecasting, with higher count of anomalous components typically correlating to larger earthquake magnitudes or shorter epicentral distances.

9. *#Avoid using Eq1 and Eq2 to refer to earthquake 1 and earthquake 2 because it easily confuses readers with equation 1 and equation 2.*

Response: Thank you for this helpful suggestion. We agree that the original notation might be confusing. Accordingly, we have replaced "Eq1" and "Eq2" with "E1" and "E2" throughout the revised manuscript to clearly distinguish the earthquake events

from equations.

10. *#The title has too much redundant information.*

Response: Thanks! We have removed the repetitive term “anomaly” and streamlined the phrasing to better reflect the core methodology.

Revised Title: [Decoding multicomponent hydrochemical anomalies: a synergetic detection model for earthquake forecasting](#)

11. *#Some corrections of language and incomplete and runoff sentences should be done before publication.*

Response: Thank you for this suggestion. We have corrected incomplete sentences and re-structured run-on sentences for better readability.